European Radiology (2021) 31:6898–6908
https://doi.org/10.1007/s00330-021-07744-w

HEPATOBILIARY-PANCREAS

Low keV portal venous phase as a surrogate for pancreatic phase in a pancreatic protocol dual-energy CT: feasibility, image quality, and lesion conspicuity

Yoshifumi Noda[1,2] · Toru Tochigi[1,3] · Anushri Parakh[1] · Evita Joseph[1] · Peter F. Hahn[1] · Avinash Kambadakone[1]

Received: 18 August 2020 / Revised: 3 January 2021 / Accepted: 4 February 2021 / Published online: 20 March 2021
© European Society of Radiology 2021

Abstract

Objective To assess the feasibility of a proposed pancreatic protocol CT generated from portal-venous phase (PVP) dual-energy CT (DECT) acquisition and its impact on image quality, lesion conspicuity, and arterial visualization/involvement.

Methods We included 111 patients (mean age, 66.8 years) who underwent pancreatic protocol DECT (pancreatic phase, PP, and PVP). The original DECT acquisition was used to create two data sets—standard protocol (50 keV PP/65 keV PVP) and proposed protocol (40 keV/65 keV PVP). Three reviewers evaluated the two data sets for image quality, lesion conspicuity, and arterial visualization/involvement using a 5-point scale. The signal-to-noise ratio (SNR) of pancreas and lesion-to-pancreas contrast-to-noise ratio (CNR) was calculated. Qualitative scores, quantitative parameters, and dose-length product (DLP) were compared between standard and proposed protocols.

Results The image quality, SNR of pancreas, and lesion-to-pancreas CNR of the standard and proposed protocol were comparable (p = 0.11–1.00). Lesion conspicuity was comparable between the standard and proposed protocols for pancreatic ductal adenocarcinoma (p = 0.55) and pancreatic cysts (p = 0.28). The visualization of larger arteries and arterial involvement were comparable between the two protocols (p = 0.056–1.00) while the scores were higher for smaller vessels in the standard protocol (p < 0.0001–0.0015). DLP of the proposed protocol (670.4 mGy·cm) showed a projected 42% reduction than the standard protocol (1145.9 mGy·cm) (p < 0.0001).

Conclusion Pancreatic protocol CT generated from a single PVP DECT acquisition is feasible and could potentially be an alternative to the standard pancreatic protocol with PP and PVP.

Key Points

- *The lesion conspicuity for focal pancreatic lesions was comparable between the proposed protocol and standard dual-phase pancreatic protocol CT.*
- *Qualitative and quantitative image assessments were almost comparable between two protocols.*
- *The radiation dose of a proposed protocol showed a projected 42% reduction from the conventional protocol.*

Keywords Pancreatic neoplasms · Multidetector-row computed tomography · Radiation dosage · Cancer screening

✉ Avinash Kambadakone
akambadakone@mgh.harvard.edu

[1] Department of Radiology, Massachusetts General Hospital, Harvard Medical School, White 270, 55 Fruit Street, White 270, Boston, MA 02114, USA

[2] Department of Radiology, Gifu University, 1-1 Yanagido, Gifu 501-1194, Japan

[3] Department of Frontier Surgery, Chiba University Graduate School of Medicine, 1-8-1 Inohana, Chuo-ku, Chiba City 260-8670, Japan

Abbreviations

ASiR	Adaptive statistical iterative reconstruction
CNR	Tumor-to-pancreas contrast-to-noise ratio
CT	Computed tomography
DECT	Dual-energy CT
DLP	Dose-length product
PDAC	Pancreatic ductal adenocarcinoma
PP	Pancreatic phase
PVP	Portal venous phase
SNR	Signal-to-noise ratio

Introduction

Multi-phasic pancreatic protocol computed tomography (CT) is considered the reference standard for initial evaluation of focal pancreatic lesions such as pancreatic ductal adenocarcinoma (PDAC) and pancreatic cystic lesions [1, 2]. This dynamic acquisition involves scanning in the pancreatic phase (PP) and portal venous phase (PVP) [3]. The PP allows improved evaluation of focal pancreatic lesions and also enables assessment of visceral arterial anatomy and their involvement by pancreatic pathologies [3, 4]. The PVP permits evaluation of porto-mesenteric vasculature and detection of focal hypodense liver lesions. In PDAC, multiphasic pancreatic protocol CT has been considered the diagnostic standard for local staging according to National Comprehensive Cancer Network (NCCN) guidelines [5]. In patients with pancreatic cysts, CT allows surveillance and assessment of internal septations, presence of solid enhancing nodules, and evaluation of main pancreatic duct. In addition, pancreatic protocol CT is valuable in screening of patients at high risk for PDAC [6]. Despite its benefits in imaging of the pancreas, one of the main concerns related to CT remains the theoretical risks related to ionizing radiation exposure particularly in patients without pancreatic malignancy and undergoing screening and surveillance exams [7].

Dual-energy CT (DECT) scanner technology allows improved tissue characterization based on their behavior at two different energy dominant spectra. A single DECT acquisition enables generation of multiple different image data sets such as monoenergetic and material specific iodine images which allows superior depiction of contrast enhancement and mitigates artifacts [8]. Low-energy monoenergetic images (40–55 keV) augment iodine density as they approximate the k-edge of iodine (33 keV) thereby allowing improved diagnosis of hypoattenuating and iso-attenuating PDAC [9, 10]. At lower kilovoltage peak (kVp) or kiloelectron volt (keV) settings, there is increased enhancement of pancreatic parenchyma and therefore higher signal-to-noise ratios (SNRs) and tumor-to-pancreas contrast-to-noise ratios (CNRs) can be obtained, compared to 65–75 keV [9]. PP monoenergetic images at 45 keV and iodine maps have been shown to improve tumor conspicuity with the optimized viewing energy level for PDAC reported to be 51 keV [11].

DECT examinations have been used to reduce radiation dose by eliminating non-contrast CT from multiphasic examinations [12]. Hybrid pancreatic protocol CT using split-bolus techniques have been proposed for evaluation of focal pancreatic lesions [7, 13]. However, there are no reported studies on a hybrid pancreatic protocol CT exploiting the low keV monoenergetic images generated from a DECT scan performed in the PVP. We hypothesized that low-energy monoenergetic images generated from a PVP DECT acquisition could be used to replace a conventional PP acquisition thereby having the benefits of two phases for one acquisition. With that goal in mind, our purpose was to study the feasibility and diagnostic performance of a novel proposed pancreatic protocol CT generated from a single-phase portal venous DECT acquisition.

Materials and methods

Patients

This retrospective study was approved by our institutional review board and the requirement for written informed consent was waived. We included 117 patients who underwent multiphasic pancreatic protocol DECT for evaluation of pancreatic pathologies between April 2016 and December 2019. Out of these 117 patients, 6 patients were excluded as they did not have a standard pancreatic protocol DECT (PP and PVP). The final cohort consisted of 111 patients (58 men and 53 women; mean age ± standard deviation [SD], 66.8 ± 13.1 years; range, 21–96 years) and included patients with PDAC (n = 48), pancreatic cystic lesions (n = 32), both PDAC and pancreatic cystic lesion (n = 5), and normal scans (n = 26) (Fig. 1). None of patients with PDAC included in this study had been treated with chemotherapy and/or radiation therapy. Detailed patient information was recorded from the medical records to document patient demographics, carbohydrate antigen (CA) 19-9 level, treatment details, endoscopy, surgical, and pathology reports.

Dual-energy CT technique

All the patients in this study underwent a pancreatic protocol DECT on a rapid kV switching DECT scanner (Discovery CT750 HD, GE Healthcare [n = 34], or Revolution CT, GE Healthcare [n = 77]). The patients were administered 80–120 mL of iodinated contrast media (Isovue 370 mg/mL, Bracco Diagnostics) at an injection rate of 3.5 mL/s followed by a 40-mL saline chaser. The PP was acquired after a fixed delay of 45 s from the start of injection, and PVP was acquired 20 s after PP acquisition. The CT imaging parameters are summarized in Table 1.

Axial plane images were reconstructed for PP monoenergetic images in 2.5-mm thickness at 50 keV and in PVP monoenergetic images in 5-mm thickness at 40 keV and 65 keV by using projection-based material decomposition software and a standard reconstruction kernel. These images were transferred to Advanced Workstation server 3.2 (GE Healthcare) and displayed with optimal window levels and widths (40 keV, 140 and 680 HU; 50 keV, 90 and 490 HU; and 65 keV, 40 and 350 HU) [14]. The dose-length product (DLP) from the dose report was recorded for each phase.

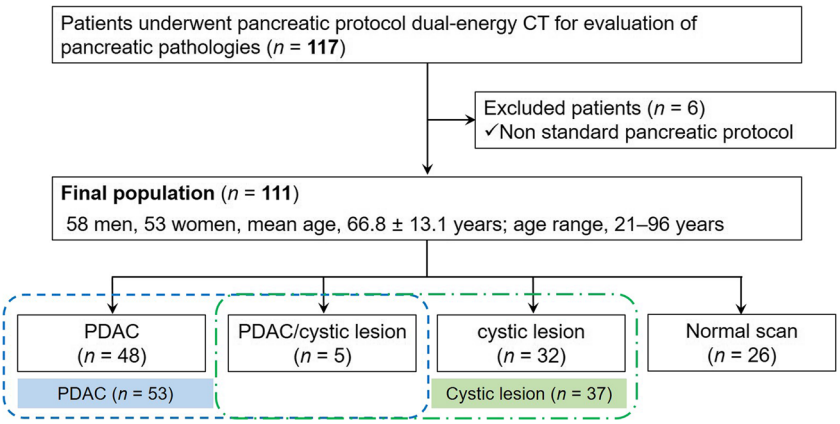

Fig. 1 Flow chart of included and excluded patients

Qualitative image analysis

Three readers (Y.N., T.T., and A.K.; 8, 12, and 15 years of post-training experience in interpreting abdominal CT images, respectively) reviewed the CT images, independently and then in consensus, using a predefined template to evaluate—the image quality, lesion conspicuity, visualization of peripancreatic arteries, and degree of arterial invasion. The image review consisted of separate sessions for the two image protocols with a 2-week time interval. During the first session, the reviewers evaluated the standard dual-phase protocol CT images (i.e., PP at 50 keV and PVP at 65 keV). In the second session, the reviewers reviewed the proposed protocol (PVP at 40 keV and PVP at 65 keV). The image quality evaluation included assessment of image noise and diagnostic acceptability using a 5-point scale: 5 = excellent; 4 = good; 3 = acceptable; 2 = suboptimal; and 1 = unacceptable.

The conspicuity of focal pancreatic lesions was graded with a 5-point scale [15]: 5 = definitely present; 4 = probably present; 3 = equivocal; 2 = probably absent; and 1 = definitely absent. A confidence score of 4 or 5 was considered definitive for the presence of focal pancreatic lesion (PDAC or pancreatic cystic lesions). The visualization of celiac, superior mesenteric, splenic, common hepatic, gastroduodenal, first jejunal arteries, and aorta, which are related to surgical resectability based on the NCCN guidelines, was graded with a 5-point scale [16]: 5 = all vascular segments from the trunk to the subsegmental peripheral artery were clearly visualized; 4 = intermediate between 5 and 3; 3 = nearly half of all vascular segments were clearly visualized; 2 = intermediate between 3 and 1; and 1 = none of the vascular segments were clearly visualized. Arterial involvement of aforementioned arteries was graded with a 5-point scale [17, 18]: 5 = deformity; 4 = encasement; 3 = abutment; 2 = hazy attenuation around the arteries; and 1 = absence of tumor contact with arteries.

Quantitative image analysis

Quantitative determination of the pancreatic parenchymal attenuation and PDAC was performed by placement of a

Table 1 Scan parameters

Parameters	Discovery CT750HD		Revolution CT
Pancreatic phase			
Patient weight	< 150 lbs	151–250 lbs	Any
mA	Fixed mA (640)	Fixed mA (600)	GSI assist
Rotation time	0.6	0.8	0.8
Pitch	1.375	1.375	0.992
Portal venous phase			
Patient weight mA	< 150 lbs Fixed mA (375)	151–250 lbs Fixed mA (630)	Same as pancreatic phase
Rotation time	0.7	0.5	
Pitch	1.375	1.375	
For both phases			
Slice/detector	40		80
Kernel	Standard		
Reconstruction	ASiR 50%		ASiR-V 50%

circular region-of interest (ROI) on PP monoenergetic images at 50 keV and PVP monoenergetic images at 40 keV to measure the CT attenuation of pancreatic parenchyma and PDAC, respectively. The estimation of pancreatic parenchymal mean CT number was performed by placing a circular ROI on the pancreatic segment downstream from the PDAC, carefully avoiding the main pancreatic duct, visible vessels, and artifacts. In those situations where placement of ROI downstream from PDAC was not possible in pancreatic head tumors, ROI placement was done upstream from the PDAC. The mean CT number of the PDAC was obtained by using a circular ROI drawn to encompass as much of the PDAC as possible on the monoenergetic images that showed the maximum PDAC diameter, carefully avoiding visible vessels and artifacts. For each monoenergetic image, 1 SD of the CT number of the homogeneous anterior abdominal wall fat tissue was defined as the background noise. The SNR of the pancreas was calculated by dividing the CT number of pancreatic parenchyma by the background noise. The CNR was calculated by the following equation: CNR = $(HU_{pancreas} - HU_{PDAC})$/background noise, where $HU_{pancreas}$ represents the mean CT number of pancreatic parenchyma and HU_{PDAC} represents that of PDAC.

Statistical analysis

Statistical analyses were performed using the MedCalc version 19.4.1 software program for Windows (MedCalc Software). The Mann–Whitney *U* test was conducted to evaluate differences in the confidence ratings for conspicuity of focal pancreatic lesions, visualization of peripancreatic arteries, degree of arterial invasion, and DLP between standard dual-phase and proposed protocols, and in the confidence ratings for image noise, diagnostic acceptability, CT numbers of pancreatic parenchyma and PDAC, background noise, SNR of the pancreas, and CNR between PP monoenergetic images at 50 keV and PVP monoenergetic images at 40 keV. The McNemar and Fisher's exact tests were performed to evaluate the differences in the sensitivity, specificity, positive predictive value (PPV), negative predictive value (NPV), and accuracy for detecting focal pancreatic lesions between standard dual-phase and proposed protocols. Interobserver variability in confidence ratings was assessed by using the κ statistics, which measure the degree of agreement between three reviewers. A κ value of $\leq$ 0.20 was interpreted as slight agreement, 0.21–0.40 as fair agreement, 0.41–0.60 as moderate agreement, 0.61–0.80 as substantial agreement, and $\geq$ 0.81 as almost perfect agreement. A p value < 0.05 was considered statistically significant.

Results

Patient demographics and tumor characteristics

Patient demographics and lesion characteristics are summarized in Table 2. Among the focal pancreatic lesions included in the study, PDACs were located in pancreatic head (n = 37), body (n = 9), and tail (n = 7) and pancreatic cysts were located in pancreatic head (n = 18), body (n = 5), and tail (n = 14). CA 19-9 level was 702.9 ± 1064.5 U/mL. Twenty-nine patients underwent surgical exploration for resection of PDAC (pancreatoduodenectomy, n = 18; distal pancreatectomy, n = 6) and R0 resection was achieved in 23 patients (79.3%). In 5 patients, locally advanced unresectable tumor was encountered during surgical exploration. Surgical resection was not performed in 24 patients. Pathological (n = 24) or clinical (n = 29) T classification was 1a in 3 patients, 1b in 1 patient, 1c in 8 patients, 2 in 29 patients, 3 in 4 patients, and 4 in 8 patients. Pathological (n = 24) or clinical (n = 29) N classification was 0 in 40 patients, 1 in 10 patients, and 2 in 3 patients. Perineural and arterial invasion were observed in 17 and 0 patients, respectively. The mean tumor size of PDAC was 29.4 ± 13.3 mm and that of the pancreatic cystic lesions was 7.0 ± 1.8 mm. All pancreatic cystic lesions included in the study had no worrisome features such as mural nodules, thickened cyst wall, or dilated main pancreatic duct.

Qualitative image analysis

Image quality and lesion conspicuity

There was no significant different in image noise (p = 0.56) and diagnostic acceptability (p = 0.13) scores in consensus between PP monoenergetic images at 50 keV and PVP monoenergetic images at 40 keV, except for the reviewer 3 during independent review (who had higher diagnostic acceptability scores of PVP monoenergetic images at 40 keV over PP monoenergetic images at 50 keV, p = 0.020) (Table 3) (Fig. 2).

The qualitative lesion conspicuity based on a 5-point confidence scale was comparable between the standard dual-phase and proposed protocols for PDAC (p = 0.55) and pancreatic cysts (p = 0.28) (Table 3). When the diagnostic performance was analyzed using a confidence score of 4 or 5 as definitive for the presence of focal pancreatic lesion, the difference between the two protocols was not statistically significant (p = 0.19–1.00). The sensitivity, specificity, PPV, NPV, and accuracy for detecting all pancreatic lesions was 94.4% (85/90), 100% (26/26), 100% (85/85), 83.9% (26/31), and 95.7% (111/116) on standard dual-phase protocol and 87.8% (79/90), 96.2% (25/26), 98.8% (79/80), 69.4% (25/36), and 89.7% (104/116) on the proposed protocol, respectively. The sensitivity, specificity, PPV, NPV, and accuracy for detecting PDAC was 94.3% (50/53), 100% (58/58), 100% (50/50), 95.1% (58/61), and 97.3% (108/111) on standard dual-phase protocol and 86.8% (46/53),

Table 2 Patient demographics and lesion characteristics

Background factors	
Age (year)	66.8 ± 13.1 (21–96)
Male:female	58:53
Body weight (kg)	70.3 ± 16.1 (41.3–112.9)
Body mass index	24.9 ± 4.8 (16.9–45.5)
PDAC location (head:body:tail)	37:9:7
Pancreatic cystic lesion location (head:body:tail)	18:5:14
CA19-9 (U/mL)	702.9 ± 1064.5 (1–3634.0)
Type of operation (PD:DP)	18:6
Surgical margin (R0:R1:R2)*	23:1:5
p/cT (1a:1b:1c:2:3:4)	3:1:8:29:4:8
p/cN (0:1:2)	40:10:3
M (0:1)	35:18
Perineural invasion (−:+)	7:17
Arterial invasion (−:+)	24:0
Tumor size of PDAC (mm)	29.4 ± 13.3 (11.6–67.4)
Size of pancreatic cystic lesion (mm)	7.0 ± 1.8 (3.6–11.3)

CA19-9 carbohydrate antigen 19-9, *PDAC* pancreatic ductal adenocarcinoma, *PD* pancreatoduodenectomy, *DP* distal pancreatectomy, *p/cT* pathological/clinical T classification, *p/cN* pathological/clinical N classification

Data are means ± 1 standard deviation with ranges in parentheses

*In 5 patients tumors were categorically unresectable during surgical exploration

98.3% (57/58), 97.9% (46/47), 89.1% (57/64), and 92.8% (103/111) on the proposed protocol, respectively; however, the different was not statistically significant (p = 0.13–1.00) (Fig. 3). The sensitivity, specificity, PPV, NPV, and accuracy for detecting pancreatic cystic lesion were 94.6% (35/37), 100% (74/74), 100% (35/35), 97.4% (74/76), and 98.2% (109/111) on standard dual-phase protocol and 89.2% (33/37), 100% (74/74), 100% (33/33), 94.9% (74/78), and 96.4% (107/111) on the proposed protocol, respectively; however, the difference was not statistically significant (p = 0.50–1.00) (Fig. 4).

Three PDACs (T1c [n = 1; confidence rating, 3 in both protocols] and T2 [n = 2; confidence ratings, 2 and 3 in both protocols] tumors) had lower confidence score for tumor conspicuity on both standard dual-phase and the proposed protocols. On the proposed protocol, four additional PDACs had a confidence score of 3 (equivocal) for lesion conspicuity. These tumors were iso-attenuating to the surrounding pancreatic parenchyma and on pathological correlation, they were T1a (n = 1) and T1c (n = 3) tumors measuring < 20 mm in size. All these tumors demonstrated mild pancreatic ductal dilatation with abrupt cutoff which resulted in them being considered suspicious on the blinded review and therefore were given a confidence score of 3. Only one case with confidence rating of 3 in standard dual-phase protocol had no PDAC but instead a pancreatic cystic lesion. Regarding pancreatic cystic lesions, two pancreatic cystic lesions (3.6 mm and 4.3 mm) were not detected in either standard dual-phase or proposed protocols. Two additional lesions (5.2 mm and 6.3 mm) were missed in the proposed protocol.

Arterial evaluation

The visualization of larger visceral arteries (celiac, superior mesenteric, and splenic arteries) was comparable between the two protocols (p = 0.056–0.56). The visualization scores of common hepatic (p = 0.0015), gastroduodenal (p < 0.0001), and first jejunal arteries (p < 0.0001) were significantly better in standard dual-phase protocol than in proposed protocol. The determination of arterial involvement scores was comparable between the two protocols (p = 0.69–1.00). The confidence scores of each reviewer and p values are shown in Tables 4 and 5. The κ value was ranged from 0.32 to 1.00, indicating fair to almost perfect agreement between the three reviewers.

Quantitative image analysis

CT numbers of the pancreas (232.3 ± 47.4 HU [133.8–373.4 HU] vs. 263.9 ± 49.5 HU [116.9–416.9 HU]; p < 0.0001) and PDAC (108.3 ± 45.7 HU [19.0–213.6 HU] vs. 166.2 ± 63.2 HU [48.7–270.4 HU]; p < 0.0001), and background noise (19.5 ± 3.6 [11.9–30.6] vs. 23.3 ± 8.0 [8.8–55.6]; p = 0.0010), were significantly greater in PVP monoenergetic images at 40 keV than in PP monoenergetic images at 50 keV. No significant different was detected in SNR of the pancreas (12.3 ± 3.4 [5.6–23.5] vs. 12.3 ± 4.0 [3.4–25.6]; p = 0.84) and CNR (6.7 ± 3.6 [0.4–19.1] vs. 5.8 ± 4.2 [0.2–25.6]; p = 0.11) between PP monoenergetic images at 50 keV and PVP monoenergetic images at 40 keV.

Radiation exposure

The mean DLP in standard dual-phase protocol are the total of those in PP and PVP. The projected mean DLP (670.4 ± 190.5 mGy·cm) in the proposed protocol were significantly lower than those in standard dual-phase protocol (mean DLP, 1145.9 ± 308.0 mGy·cm) (p < 0.0001). An average reduction rate of mean DLP and case-based reduction rate of DLP were 41.5% and 41.2% (range, 28.6–71.5%), respectively.

Discussion

Multiphasic pancreatic protocol CT is the initial imaging modality of choice in the evaluation of patients with suspected focal cystic or solid pancreatic lesions. While radiation dose reduction is not a consideration in patients with malignancies such as PDAC, a low-dose pancreatic protocol CT is desirable in patients without malignant pancreatic processes, for example, in

Table 3 Image quality and tumor conspicuity in standard dual-phase and proposed protocols

	Standard dual-phase protocol (PP images at 50 keV)†		Proposed protocol (PVP images at 40 keV) †		*p* value (confidence rating)
	Confidence rating	κ value	Confidence rating	κ value	
Image noise†	3.9 ± 0.4 (2–5)		3.9 ± 0.4 (2–5)		0.56
Reader 1	3.9 ± 0.4 (2–5)	0.69 (R1 vs. R2)	3.9 ± 0.4 (2–5)	0.90 (R1 vs. R2)	0.43
Reader 2	3.9 ± 0.4 (2–5)	0.53 (R2 vs. R3)	3.9 ± 0.4 (2–5)	0.51 (R2 vs. R3)	0.71
Reader 3	3.9 ± 0.5 (2–5)	0.55 (R1 vs. R3)	4.0 ± 0.5 (2–5)	0.49 (R1 vs. R3)	0.10
Diagnostic acceptability†	4.0 ± 0.3 (2–5)		3.9 ± 0.3 (2–5)		0.13
Reader 1	4.0 ± 0.3 (2–5)	0.82 (R1 vs. R2)	3.9 ± 0.3 (2–5)	0.95 (R1 vs. R2)	0.20
Reader 2	4.0 ± 0.3 (3–5)	0.41 (R2 vs. R3)	3.9 ± 0.3 (2–5)	0.30 (R2 vs. R3)	0.13
Reader 3	4.0 ± 0.5 (2–5)	0.36 (R1 vs. R3)	4.2 ± 0.6 (2–5)	0.29 (R1 vs. R3)	0.020*
Conspicuity of PDAC	2.8 ± 1.9 (1–5)		2.7 ± 1.8 (1–5)		0.55
Reader 1	2.8 ± 1.9 (1–5)	0.91 (R1 vs. R2)	2.7 ± 1.8 (1–5)	0.92 (R1 vs. R2)	0.53
Reader 2	2.8 ± 1.9 (1–5)	0.96 (R2 vs. R3)	2.7 ± 1.8 (1–5)	0.90 (R2 vs. R3)	0.50
Reader 3	2.8 ± 1.9 (1–5)	0.95 (R1 vs. R3)	2.8 ± 1.9 (1–5)	0.88 (R1 vs. R3)	0.87
Conspicuity of pancreatic cystic lesion	2.4 ± 1.7 (1–5)		2.1 ± 1.6 (1–5)		0.28
Reader 1	2.3 ± 1.7 (1–5)	0.98 (R1 vs. R2)	2.1 ± 1.6 (1–5)	0.99 (R1 vs. R2)	0.41
Reader 2	2.3 ± 1.7 (1–5)	0.83 (R2 vs. R3)	2.1 ± 1.6 (1–5)	0.81 (R2 vs. R3)	0.40
Reader 3	2.3 ± 1.8 (1–5)	0.86 (R1 vs. R3)	2.3 ± 1.8 (1–5)	0.81 (R1 vs. R3)	0.88

PP pancreatic phase, *PVP* portal venous phase, *PDAC* pancreatic ductal adenocarcinoma, *N.A.* not applicable

Data are means ± 1 standard deviation with ranges in parentheses

*$p < 0.05$, significant difference

† Image quality was compared between PP monoenergetic images at 50 keV and PVP monoenergetic images at 40 keV

patients undergoing follow-up imaging surveillance for pancreatic cysts and in screening evaluation of patients at high risk for PDAC such as those with new-onset diabetes mellitus. We investigated a novel pancreatic protocol CT with the PP generated from a single PVP DECT acquisition and found that this proposed protocol is feasible and could potentially be an alternative to the standard dual-phase pancreatic protocol CT for routine evaluation of focal pancreatic lesions with comparable diagnostic performance. The elimination of the PP showed significant projected radiation dose reduction of 44%.

Qualitative determination of lesion conspicuity on PVP monoenergetic images at 40 keV for both solid and cystic pancreatic lesions was comparable to the PP monoenergetic images at 50 keV. The pooled diagnostic performance for detecting focal pancreatic lesions in our cohort which included 26 normal scans was comparable between the standard dual-phase and proposed protocols. The lower sensitivity scores for diagnosis of focal pancreatic lesions is due to our strict criteria for definitive lesion detection based on the confidence scores; i.e., we used only those lesions with a confidence score of 4 or 5 as definitive for presence of a lesion. The four PDACs with lower conspicuity scores on the PVP monoenergetic images at 40 keV were tumors measuring < 20 mm and iso-attenuating to the surrounding pancreatic parenchyma. However, presence of

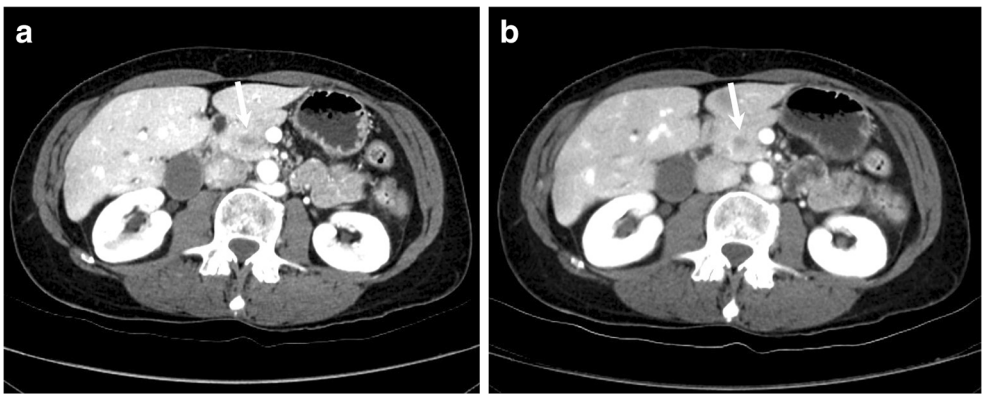

Fig. 2 **a** Axial pancreatic phase monochromatic image at 50 keV and (**b**) axial portal venous phase monochromatic image at 40 keV show comparable image quality. Pancreatic ductal adenocarcinoma (arrow) is also well visualized

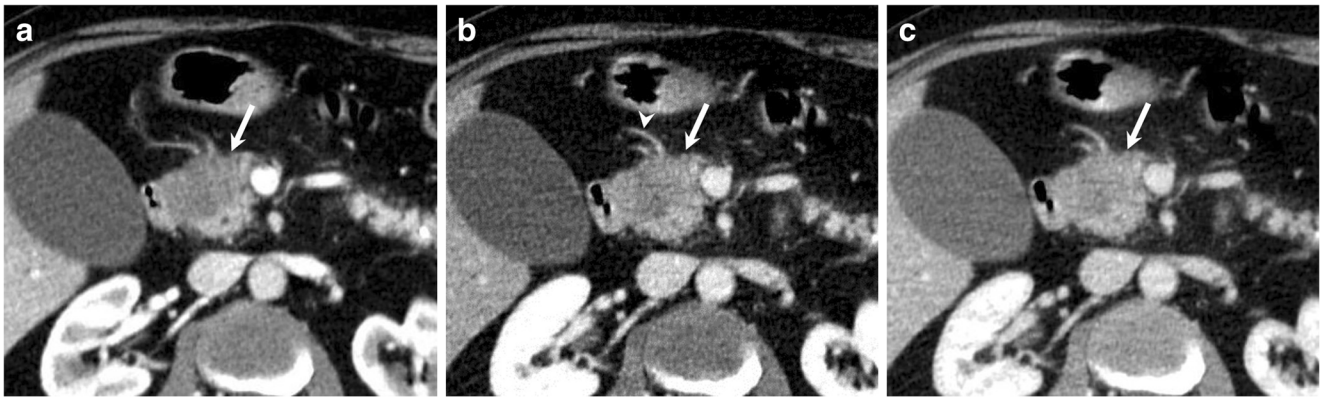

Fig. 3 A 68-year-old female with pancreatic ductal adenocarcinoma (PDAC) in the pancreatic head. **a** Axial pancreatic phase (PP) monochromatic image at 50 keV, (**b**) axial portal venous phase (PVP) monochromatic image at 40 keV, and (**c**) axial PVP monochromatic image at 65 keV show hypovascular PDAC (arrow). The visualization of PDAC is comparable between 50 keV PP (**a**) and 40 keV PVP (**b**) monochromatic images

additional features such as main pancreatic ductal dilatation and abrupt duct-off allowed their identification and an equivocal confidence score of 3 on the blinded review. The sensitivity of CT for detecting PDAC has been reported to be 86–89% [19, 20] and the sensitivity falls to 70% for lesions < 20 mm in size [19]. Based on prior published literature on detection of PDAC, the sensitivity for detecting PDAC of our proposed protocol was comparable despite the rigorous criteria (86.8%).

We found that the visualization of large arteries such as the celiac, superior mesenteric, and splenic arteries, the degree of arterial invasion, image quality, SNR of the pancreas, and CNR were not significantly different between the standard dual-phase and proposed protocols. On the other hand, the visualization of small arteries including common hepatic, gastroduodenal, and first jejunal arteries was significantly better in standard dual-phase protocol compared to the proposed protocol. However, there was no significant difference in the determination of arterial involvement between the two protocols. Therefore, we believe that the proposed protocol maintains the ability of the reader to accurately evaluate arterial involvement on the PVP monoenergetic images at 40 keV without affecting the assessment of tumor resectability.

Although image quality was comparable between PP monoenergetic images at 50 keV and PVP monoenergetic images at 40 keV, the confidence score was slightly lower, and background noise was significantly greater for PVP monoenergetic images at 40 keV compared with PP monoenergetic images at 50 keV. At lower energy levels, monoenergetic image reconstruction is associated with increasing beam-hardening artifacts, often leading to reduction in image quality compared with conventional image reconstruction [21]. Moreover, spatial resolution is also decreased in monoenergetic images reconstruction at lower energy levels, which affects the visualization of small arteries [22]. However, the newer generation rapid-kilovoltage-switching DECT can reduce beam-hardening artifacts and improve spatial resolution at lower energy levels [23]. Additionally, a new generation reconstruction technique, ASiR-V, has been applied for several clinical settings which improves the objective and subjective image quality compared with ASiR [24–27]. In our

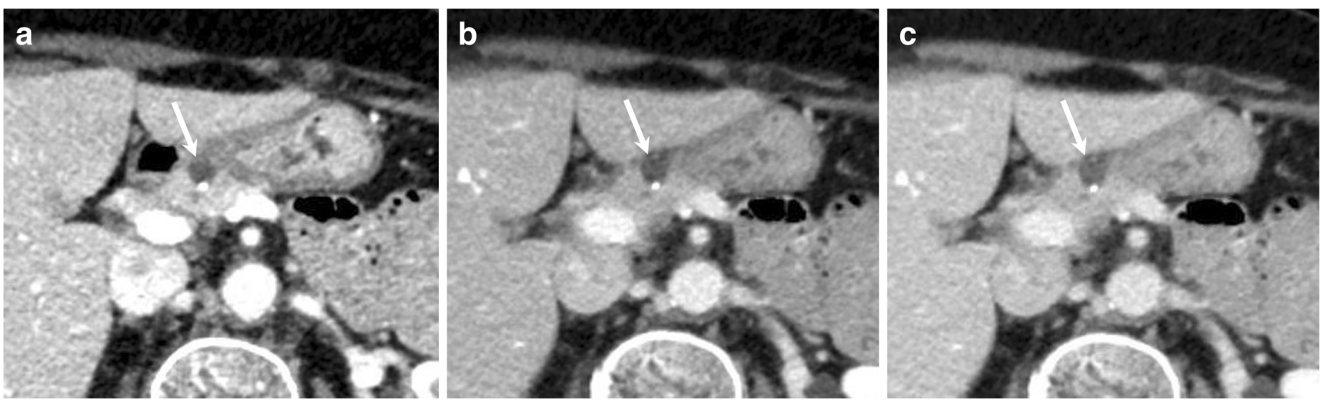

Fig. 4 A 64-year-old female with pancreatic cystic lesion in the head. **a** Axial pancreatic phase (PP) monochromatic image at 50 keV, (**b**) axial portal venous phase (PVP) monochromatic image at 40 keV, and (**c**) axial PVP monochromatic image at 65 keV show well-defined cystic lesion (arrow). The visualization of pancreatic cystic lesion is comparable between 50 keV PP (**a**) and 40 keV PVP (**b**) monochromatic images

Table 4 Arterial visualization in standard dual-phase and proposed protocols

	Standard dual-phase protocol		Proposed protocol		*p* value (confidence rating)
	Confidence rating	κ value	Confidence rating	κ value	
Celiac artery	5.0 (5)		4.9 ± 0.1 (4–5)		0.32
Reader 1	5.0 (5)	1.00 (R1 vs. R2)	4.9 ± 0.1 (4–5)	1.00 (R1 vs. R2)	0.32
Reader 2	5.0 (5)	1.00 (R2 vs. R3)	4.9 ± 0.1 (4–5)	0.39 (R2 vs. R3)	0.32
Reader 3	5.0 (5)	1.00 (R1 vs. R3)	4.9 ± 0.4 (4–5)	0.39 (R1 vs. R3)	0.024*
Superior mesenteric artery	4.9 ± 0.1 (4–5)		4.9 ± 0.1 (4–5)		0.56
Reader 1	4.9 ± 0.1 (4–5)	1.00 (R1 vs. R2)	4.9 ± 0.1 (4–5)	0.85 (R1 vs. R2)	0.56
Reader 2	4.9 ± 0.1 (4–5)	1.00 (R2 vs. R3)	4.9 ± 0.2 (3–5)	0.39 (R2 vs. R3)	0.56
Reader 3	5.0 (5)	1.00 (R1 vs. R3)	4.9 ± 0.4 (3–5)	0.32 (R1 vs. R3)	0.044*
Splenic artery	4.9 ± 0.2 (4–5)		4.8 ± 0.5 (2–5)		0.056
Reader 1	4.9 ± 0.2 (4–5)	0.65 (R1 vs. R2)	4.8 ± 0.5 (2–5)	0.96 (R1 vs. R2)	0.056
Reader 2	4.9 ± 0.2 (4–5)	0.79 (R2 vs. R3)	4.8 ± 0.5 (2–5)	0.51 (R2 vs. R3)	0.009*
Reader 3	4.9 ± 0.2 (4–5)	0.56 (R1 vs. R3)	4.8 ± 0.7 (1–5)	0.51 (R1 vs. R3)	0.023*
Common hepatic artery	4.9 ± 0.4 (1–5)		4.7 ± 0.7 (1–5)		0.0015*
Reader 1	4.9 ± 0.4 (1–5)	0.85 (R1 vs. R2)	4.7 ± 0.7 (1–5)	0.95 (R1 vs. R2)	0.0005*
Reader 2	4.9 ± 0.4 (1–5)	0.66 (R2 vs. R3)	4.7 ± 0.7 (1–5)	0.56 (R2 vs. R3)	0.0002*
Reader 3	4.9 ± 0.2 (4–5)	0.56 (R1 vs. R3)	4.7 ± 0.8 (1–5)	0.63 (R1 vs. R3)	< 0.0001*
Gastroduodenal artery	4.6 ± 1.0 (1–5)		4.1 ± 1.1 (1–5)		< 0.0001*
Reader 1	4.6 ± 0.9 (1–5)	0.99 (R1 vs. R2)	4.1 ± 1.1 (1–5)	0.96 (R1 vs. R2)	< 0.0001*
Reader 2	4.6 ± 1.0 (1–5)	0.63 (R2 vs. R3)	4.0 ± 1.1 (1–5)	0.66 (R2 vs. R3)	< 0.0001*
Reader 3	4.7 ± 0.8 (1–5)	0.65 (R1 vs. R3)	4.1 ± 1.1 (1–5)	0.60 (R1 vs. R3)	< 0.0001*
First jejunal artery	4.7 ± 0.7 (1–5)		4.2 ± 1.1 (1–5)		< 0.0001*
Reader 1	4.7 ± 0.7 (1–5)	0.97 (R1 vs. R2)	4.2 ± 1.1 (1–5)	0.97 (R1 vs. R2)	< 0.0001*
Reader 2	4.7 ± 0.7 (1–5)	0.80 (R2 vs. R3)	4.1 ± 1.1 (1–5)	0.80 (R2 vs. R3)	< 0.0001*
Reader 3	4.8 ± 0.7 (1–5)	0.63 (R1 vs. R3)	4.4 ± 1.0 (1–5)	0.63 (R1 vs. R3)	0.0002*
Aorta	5 (5)		5 (5)		1.00
Reader 1	5 (5)	1.00 (R1 vs. R2)	5 (5)	1.00 (R1 vs. R2)	1.00
Reader 2	5 (5)	1.00 (R2 vs. R3)	5 (5)	1.00 (R2 vs. R3)	1.00
Reader 3	5 (5)	1.00 (R1 vs. R3)	5 (5)	1.00 (R1 vs. R3)	1.00

N.A. not applicable

Data are means ± 1 standard deviation with ranges in parentheses

*$p < 0.05$, significant difference

study, approximately one-third of cases were scanned by Discovery CT750HD, an earlier generation scanner compared to Revolution CT, and we applied ASiR of 50% for all patients scanned by Discovery CT750HD because of the retrospective study design. Newer technological innovations potentially could improve image quality and visualization of small arteries.

Diagnostic reference levels (DRLs) and achievable dose (AD) are the performance parameters for radiation protection and optimization of patient imaging [28]. DRLs and AD are typically set to the 75th and 50th percentile of the dose distribution based on a survey [29]. The developed DRLs and AD for the abdomen and pelvis with contrast material were 15 mGy and 12 mGy in CTDIvol, and 755 mGy·cm and 608 mGy·cm in DLP [29]. AD was almost reached when applying the proposed pancreatic protocol for patients with PDAC.

Rising use of cross-section imaging has led to increasing detection of pancreatic cysts and follow-up imaging with contrast-enhanced pancreatic protocol CT or MRI is being recommended by multiple organizations for surveillance of pancreatic cysts to identify worrisome features or PDAC [30]. Pancreatic surveillance or screening for PDAC is recommended in select high-risk individuals with family history or genetic predisposition, or in those patients with new-onset diabetes mellitus [31, 32]. While pancreatic protocol CT and MRI are comparable for detecting worrisome features in pancreatic cysts or diagnosis of PDAC, one of the limitations of CT is the cumulative radiation exposure related to multiple follow-up CT scans [30]. Previous studies have investigated the efficacy of hybrid CT protocols such as split bolus techniques which incorporate splitting of the contrast material injection and obtaining multiple contrast phases in a single scan [7, 13]. Split-bolus pancreatic protocol CT allows radiation dose reduction while maintaining image quality and tumor conspicuity but would require additional dose of contrast bolus which is not desirable in patients with borderline renal insufficiency [33]. Our proposed protocol allows creation of a PP from a low keV PVP acquisition with similar diagnostic performance to a dual-phase acquisition without additional intravenous contrast dose. This novel technique would be a valuable tool in pancreatic screening and surveillance of patients with pancreatic cysts.

Our study has several limitations. First, this was a retrospective study with a small sample size which could

Table 5 Arterial involvement in standard dual-phase and proposed protocols

	Standard dual-phase protocol		Proposed protocol		*p* value (confidence rating)
	Confidence rating	κ value	Confidence rating	κ value	
Celiac artery	1.2 ± 0.8 (1–5)		1.2 ± 0.8 (1–5)		1.00
Reader 1	1.2 ± 0.8 (1–5)	0.99 (R1 vs. R2)	1.2 ± 0.8 (1–5)	1.00 (R1 vs. R2)	0.81
Reader 2	1.2 ± 0.8 (1–5)	0.96 (R2 vs. R3)	1.2 ± 0.8 (1–5)	0.86 (R2 vs. R3)	0.99
Reader 3	1.2 ± 0.9 (1–5)	0.95 (R1 vs. R3)	1.3 ± 0.9 (1–5)	0.86 (R1 vs. R3)	0.63
Superior mesenteric artery	1.5 ± 1.0 (1–5)		1.4 ± 1.0 (1–5)		0.69
Reader 1	1.4 ± 1.0 (1–5)	0.98 (R1 vs. R2)	1.4 ± 1.0 (1–5)	0.99 (R1 vs. R2)	0.89
Reader 2	1.4 ± 1.0 (1–5)	0.94 (R2 vs. R3)	1.4 ± 1.0 (1–5)	0.89 (R2 vs. R3)	0.72
Reader 3	1.4 ± 1.0 (1–5)	0.93 (R1 vs. R3)	1.4 ± 1.1 (1–5)	0.91 (R1 vs. R3)	0.82
Splenic artery	1.4 ± 1.2 (1–5)		1.4 ± 1.2 (1–5)		1.00
Reader 1	1.4 ± 1.2 (1–5)	0.99 (R1 vs. R2)	1.4 ± 1.2 (1–5)	1.00 (R1 vs. R2)	1.00
Reader 2	1.4 ± 1.1 (1–5)	0.95 (R2 vs. R3)	1.4 ± 1.2 (1–5)	0.90 (R2 vs. R3)	0.99
Reader 3	1.5 ± 1.2 (1–5)	0.93 (R1 vs. R3)	1.5 ± 1.3 (1–5)	0.90 (R1 vs. R3)	0.53
Common hepatic artery	1.3 ± 0.9 (1–5)		1.3 ± 0.9 (1–5)		1.00
Reader 1	1.3 ± 0.9 (1–5)	0.88 (R1 vs. R2)	1.3 ± 0.9 (1–5)	0.95 (R1 vs. R2)	0.88
Reader 2	1.3 ± 0.9 (1–5)	0.89 (R2 vs. R3)	1.3 ± 0.9 (1–5)	0.79 (R2 vs. R3)	0.88
Reader 3	1.3 ± 0.9 (1–5)	0.90 (R1 vs. R3)	1.4 ± 1.0 (1–5)	0.83 (R1 vs. R3)	0.56
Gastroduodenal artery	1.8 ± 1.4 (1–5)		1.7 ± 1.4 (1–5)		0.97
Reader 1	1.8 ± 1.4 (1–5)	0.92 (R1 vs. R2)	1.7 ± 1.4 (1–5)	0.96 (R1 vs. R2)	0.93
Reader 2	1.7 ± 1.4 (1–5)	0.89 (R2 vs. R3)	1.8 ± 1.4 (1–5)	0.90 (R2 vs. R3)	0.91
Reader 3	1.8 ± 1.5 (1–5)	0.89 (R1 vs. R3)	1.8 ± 1.4 (1–5)	0.89 (R1 vs. R3)	0.91
First jejunal artery	1.3 ± 1.0 (1–5)		1.3 ± 1.0 (1–5)		0.84
Reader 1	1.3 ± 1.0 (1–5)	0.97 (R1 vs. R2)	1.3 ± 1.0 (1–5)	1.00 (R1 vs. R2)	0.84
Reader 2	1.3 ± 0.9 (1–5)	0.93 (R2 vs. R3)	1.3 ± 1.0 (1–5)	0.82 (R2 vs. R3)	0.82
Reader 3	1.3 ± 0.9 (1–5)	0.91 (R1 vs. R3)	1.4 ± 1.1 (1–5)	0.82 (R1 vs. R3)	0.66
Aorta	1.1 ± 0.4 (1–3)		1.1 ± 0.4 (1–3)		1.00
Reader 1	1.1 ± 0.4 (1–3)	1.00 (R1 vs. R2)	1.1 ± 0.4 (1–3)	1.00 (R1 vs. R2)	1.00
Reader 2	1.1 ± 0.4 (1–3)	0.85 (R2 vs. R3)	1.1 ± 0.4 (1–3)	0.74 (R2 vs. R3)	1.00
Reader 3	1.1 ± 0.3 (1–3)	0.85 (R1 vs. R3)	1.1 ± 0.4 (1–3)	0.74 (R1 vs. R3)	0.70

N.A. not applicable

Data are means ± 1 standard deviation with ranges in parentheses

result in selection bias. A non-inferiority design comparing the proposed protocol with the standard dual-phase pancreatic protocol could not be performed as a significantly larger sample size would be needed to validate the results. However, as our study reports the feasibility of using a single PVP for creation of dual-phase pancreatic protocol CT, future studies in larger cohorts could be performed. Secondly, the slice thickness was different between PP (2.5 mm) and PVP (5 mm) monoenergetic images. This difference probably affects the slightly lower confidence scores for conspicuity of focal pancreatic lesions, visualization of small arteries, and background noise. Third, patients scanned on two different rapid-kilovoltage-switching DECT scanners were included in the study (Discovery CT750 HD and Revolution CT, GE Healthcare). CT numbers of the liver (121.9 HU vs. 123.1 HU) and pancreas (101.9 HU vs. 110.1 HU) in PVP were not so different between Discovery CT750 HD and Revolution CT according to previous reports [14, 34]. Given the similar DECT technology, the variation of scanners would have had no more than minimal impact on the study results. Finally, we only used rapid-kilovoltage-switching DECT scanners from a single vendor. Therefore, further clinical studies with a larger sample size and unified slice thickness are required to validate our results for other DECT scanners such as dual-source or multi-layer spectral DECT.

In conclusion, a proposed pancreatic protocol CT generated from a single PVP DECT acquisition is feasible and can potentially be an alternative to the standard dual-phase acquisition. This proposed protocol has the potential in patients with suspected pancreatic disease or benign pancreatic processes or those patients undergoing repeated imaging evaluation for screening of pancreatic malignancy.

Funding AK: Grant support for research activities from Philips and GE Healthcare. Other authors report no relevant disclosures or conflicts of interest.

Declarations

Guarantor The scientific guarantor of this publication is Avinash Kambadakone.

Conflict of interest AK: Grant support for research activities from Philips, GE Healthcare and PanCAN. Other authors report no relevant disclosures or conflicts of interest.

Statistics and biometry No complex statistical methods were necessary for this paper.

Informed consent Written informed consent was obtained from all subjects (patients) in this study.

Ethical approval Institutional Review Board approval was obtained.

Methodology
- Retrospective
- Diagnostic or prognostic study
- Performed at one institution

References

1. Klauss M, Schobinger M, Wolf I et al (2009) Value of three-dimensional reconstructions in pancreatic carcinoma using multidetector CT: initial results. World J Gastroenterol 15:5827–5832
2. Lee JE, Choi SY, Min JH et al (2019) Determining malignant potential of intraductal papillary mucinous neoplasm of the pancreas: CT versus MRI by using Revised 2017 International Consensus Guidelines. Radiology 293:134–143
3. Lu DS, Vedantham S, Krasny RM, Kadell B, Berger WL, Reber HA (1996) Two-phase helical CT for pancreatic tumors: pancreatic versus hepatic phase enhancement of tumor, pancreas, and vascular structures. Radiology 199:697–701
4. Lu DS, Reber HA, Krasny RM, Kadell BM, Sayre J (1997) Local staging of pancreatic cancer: criteria for unresectability of major vessels as revealed by pancreatic-phase, thin-section helical CT. AJR Am J Roentgenol 168:1439–1443
5. NCCN clinical practice guidelines in oncology: pancreatic adenocarcinoma, version 3. 2019. https://www.nccn.org/professionals/physician_gls/pdf/pancreaticpdf
6. Pandey P, Pandey A, Luo Y et al (2019) Follow-up of incidentally detected pancreatic cystic neoplasms: do baseline MRI and CT features predict cyst growth? Radiology 292:647–654
7. Brook OR, Gourtsoyianni S, Brook A, Siewert B, Kent T, Raptopoulos V (2013) Split-bolus spectral multidetector CT of the pancreas: assessment of radiation dose and tumor conspicuity. Radiology 269:139–148
8. Noda Y, Goshima S, Miyoshi T et al (2018) Assessing chemotherapeutic response in pancreatic ductal adenocarcinoma: histogram analysis of iodine concentration and CT number in single-source dual-energy CT. AJR Am J Roentgenol 211:1221–1226
9. Noda Y, Goshima S, Kaga T et al (2019) Virtual monochromatic image at lower energy level for assessing pancreatic ductal adenocarcinoma in fast kV-switching dual-energy CT. Clin Radiol. https://doi.org/10.1016/j.crad.2019.11.012
10. Ohira S, Kanayama N, Wada K et al (2019) A third-generation adaptive statistical iterative reconstruction for contrast-enhanced 4-dimensional dual-energy computed tomography for pancreatic cancer. J Comput Assist Tomogr. https://doi.org/10.1097/RCT.0000000000000942
11. Aslan S, Camlidag I, Nural MS (2019) Lower energy levels and iodine-based material decomposition images increase pancreatic ductal adenocarcinoma conspicuity on rapid kV-switching dual-energy CT. Abdom Radiol (NY) 44:568–575
12. Sauter AP, Muenzel D, Dangelmaier J et al (2018) Dual-layer spectral computed tomography: virtual non-contrast in comparison to true non-contrast images. Eur J Radiol 104:108–114
13. Camacho A, Fang J, Cohen MP, Raptopoulos V, Brook OR (2018) Split-bolus pancreas CTA protocol for local staging of pancreatic cancer and detection and characterization of liver lesions. Abdom Radiol (NY) 43:340–350
14. Noda Y, Goshima S, Kozaka K et al (2018) Optimal window settings in single-source dual-energy computed tomography of the abdomen. Eur J Radiol 109:204–209
15. Noda Y, Kanematsu M, Goshima S et al (2014) Reduction of iodine load in CT imaging of pancreas acquired with low tube voltage and an adaptive statistical iterative reconstruction technique. J Comput Assist Tomogr 38:714–720
16. Noda Y, Goshima S, Koyasu H et al (2017) Renovascular CT: comparison between adaptive statistical iterative reconstruction and model-based iterative reconstruction. Clin Radiol 72:901 e913–901 e919. https://doi.org/10.1016/j.crad.2017.06.002
17. Hong SB, Lee SS, Kim JH et al (2018) Pancreatic cancer CT: prediction of resectability according to NCCN Criteria. Radiology 289:710–718
18. Al-Hawary MM, Francis IR, Chari ST et al (2014) Pancreatic ductal adenocarcinoma radiology reporting template: consensus statement of the Society of Abdominal Radiology and the American Pancreatic Association. Radiology 270:248–260
19. Tamm EP, Loyer EM, Faria SC, Evans DB, Wolff RA, Charnsangavej C (2007) Retrospective analysis of dual-phase MDCT and follow-up EUS/EUS-FNA in the diagnosis of pancreatic cancer. Abdom Imaging 32:660–667. https://doi.org/10.1007/s00261-007-9298-x
20. DeWitt J, Devereaux B, Chriswell M et al (2004) Comparison of endoscopic ultrasonography and multidetector computed tomography for detecting and staging pancreatic cancer. Ann Intern Med 141:753–763
21. Wu R, Watanabe Y, Satoh K et al (2018) Quantitative comparison of virtual monochromatic images of dual energy computed tomography systems: beam hardening artifact correction and variance in computed tomography numbers: a phantom study. J Comput Assist Tomogr 42:648–654
22. Sugawara H, Suzuki S, Katada Y et al (2019) Comparison of full-iodine conventional CT and half-iodine virtual monochromatic imaging: advantages and disadvantages. Eur Radiol 29:1400–1407
23. Sugawara H, Takayanagi T, Ishikawa T et al (2019) New fast kVp switching dual-energy CT: reduced severity of beam hardening artifacts and improved image quality in reduced-iodine virtual monochromatic imaging. Acad Radiol. https://doi.org/10.1016/j.acra.2019.11.015
24. Han WK, Na JC, Park SY (2020) Low-dose CT angiography using ASiR-V for potential living renal donors: a prospective analysis of image quality and diagnostic accuracy. Eur Radiol 30:798–805
25. Tang H, Liu Z, Hu Z et al (2019) Clinical value of a new generation adaptive statistical iterative reconstruction (ASIR-V) in the diagnosis of pulmonary nodule in low-dose chest CT. Br J Radiol 92:20180909. https://doi.org/10.1259/bjr.20180909
26. Chen Y, Liu Z, Li M et al (2019) Reducing both radiation and contrast doses in coronary CT angiography in lean patients on a 16-cm wide-detector CT using 70 kVp and ASiR-V algorithm, in comparison with the conventional 100-kVp protocol. Eur Radiol 29:3036–3043
27. Chen LH, Jin C, Li JY et al (2018) Image quality comparison of two adaptive statistical iterative reconstruction (ASiR, ASiR-V) algorithms and filtered back projection in routine liver CT. Br J Radiol 91:20170655. https://doi.org/10.1259/bjr.20170655
28. (1991) 1990 Recommendations of the International Commission on Radiological Protection. Ann ICRP 21:1–201

29. Kanal KM, Butler PF, Sengupta D, Bhargavan-Chatfield M, Coombs LP, Morin RL (2017) U.S. diagnostic reference levels and achievable doses for 10 adult CT examinations. Radiology 284:120–133
30. Megibow AJ, Baker ME, Morgan DE et al (2017) Management of incidental pancreatic cysts: a white paper of the ACR Incidental Findings Committee. J Am Coll Radiol 14:911–923
31. Goggins M, Overbeek KA, Brand R et al (2020) Management of patients with increased risk for familial pancreatic cancer: updated recommendations from the International Cancer of the Pancreas Screening (CAPS) Consortium. Gut 69:7–17
32. Maitra A, Sharma A, Brand RE et al (2018) A prospective study to establish a new-onset diabetes cohort: from the consortium for the study of chronic pancreatitis, diabetes, and pancreatic cancer. Pancreas 47:1244–1248
33. Muenzfeld H, Mahjoub S, Roehle R et al (2019) Split-bolus vs. multiphasic contrast bolus protocol in patients with pancreatic cancer or cholangiocarcinoma. Eur J Radiol 119:108626. https://doi.org/10.1016/j.ejrad.2019.07.027
34. Noda Y, Goshima S, Nakashima Y et al (2020) Iodine dose optimization in portal venous phase virtual monochromatic images of the abdomen: Prospective study on rapid kVp switching dual energy CT. Eur J Radiol 122:108746

Publisher's note Springer Nature remains neutral with regard to jurisdictional claims in published maps and institutional affiliations.